COMMUNICATIONS IN COMPUTATIONAL PHYSICS
Vol. **1**, No. 5, pp. 827-846

Commun. Comput. Phys.
October 2006

Numerical Simulation of Compositional Flow in Porous Media under Gravity

Zhangxin Chen[1,2,3,*], Guoqiang (Joe) Zhou[4] and Dan Carruthers[4]

[1] *Center for Scientific Computation, Southern Methodist University, Dallas, TX 75275-0156, USA.*
[2] *Research Center for Science, Xi'an Jiaotong University, Xi'an 710049, P. R. China.*
[3] *Center for Advanced Reservoir Modeling and Simulation, College of Engineering, Peking University, P. R. China.*
[4] *The Permedia Research Group, 577 Somerset St. W., Ottawa, Ontario K1R 5K1, Canada.*

Received 9 November 2005; Accepted (in revised version) 15 March 2006

Abstract. This paper is concerned with the numerical simulation of multiphase, multicomponent flow in porous media. The model equations are based on compositional flow with mass interchange between phases. The compositional model consists of Darcy's law for volumetric flow velocities, mass conservation for hydrocarbon components, thermodynamic equilibrium for mass interchange between phases, and an equation of state for saturations. High-accurate finite volume methods on unstructured grids are used to discretize the model governing equations. Special emphasis is placed on studying the influence of gravitational effects on the overall displacement dynamics. In particular, free and forced convections, diffusions, and dispersions are studied in separate and combined cases, and their interplays are intensively analyzed for gravitational instabilities. Extensive numerical experiments are presented to validate the numerical study under consideration.

Key words: Compositional model; reservoir simulation; finite volume method; unstructured grids; gravitational effect; free and forced convections; diffusions; dispersions; numerical experiments.

1 Introduction

This paper is concerned with the numerical simulation of multiphase, multicomponent compositional model often used in petroleum reservoirs. This model incorporates compressibility, compositional effects, and mass interchange between phases. It consists of

*Correspondence to: Zhangxin Chen, Center for Scientific Computation, Southern Methodist University, Dallas, TX 75275-0156, USA. Email: zchen@mail.smu.edu

Darcy's law for volumetric flow velocities, mass conservation for hydrocarbon components, thermodynamic equilibrium for mass interchange between phases, and an equation of state for saturations. It models important hydrocarbon recovery processes such as natural depletion or gas cycling drive for gas condensate reservoirs and miscible flooding for volatile oil reservoirs. To understand complex thermodynamic and physical phenomena of multiphase flow in petroleum reservoirs, it has become increasingly important to simulate numerically such a realistic model.

A qualitative analysis of the compositional model under consideration was given in [6, 14]. The mathematical structure of the differential system describing this model was studied, and numerical results were given for a one-dimensional version of this model. Three-dimensional simulations of the compositional model using finite difference and finite element methods were presented in [4, 5]. In this paper, we present numerical results for the three-dimensional compositional model using high-accurate finite volume methods on unstructured grids, with an emphasis on the numerical study of interfacial instabilities under gravitational forces. An implicit second-order integration scheme is exploited for time differentiation terms, the Newton-Raphson iteration is utilized for linearization, and the BiCGSTAB (biconjugate gradient stabilized) iterative algorithm with ILU preconditioners is employed for the solution of linear systems.

Fluid flow models in porous media involve large systems of nonlinear, coupled, time-dependent partial differential equations. An important problem in reservoir simulation is to develop stable, efficient, robust, and accurate solution approaches for solving these coupled equations. Essentially, there are three types of solution approaches in reservoir simulation: the IMPES (implicit in pressure and explicit in saturation), the fully implicit, and the sequential. The fully implicit solution approach, which is also called the simultaneous solution approach [7], solves all of the coupled nonlinear equations simultaneously. This approach is stable and can take very large time steps, while its stability is maintained. However, due to a large number of partial differential equations to solve for the compositional model, this solution approach is computationally prohibitive, even on today's most powerful supercomputers. The sequential solution approach [10] splits the coupled system of nonlinear governing equations of reservoir simulation up into individual equations and solves each of these equations separately and implicitly. This approach is less stable but more efficient than the fully implicit approach for the compositional model, and will be investigated in our future study for this model. In the present paper, by a careful choice of the primary unknowns an *iterative* IMPES solution approach is employed to solve the system of the compositional governing equations.

As an application of the solution approach developed here, the stability of interfaces separating fluids of different densities and viscosities in porous media is studied. By means of experiments and, more recently, numerical simulations, the nonlinear interfacial dynamics has been studied using a variety of physical models and geometries [9]. In many reservoir applications, the basic instability is due to the density and viscosity contrast and permeability (conductivity) variations. In this paper, the nonlinear evolution of interfaces between miscible fluids of different densities is particularly analyzed. Both forced convec-

tion (i.e., transport driven by a hydraulic gradient) and free convection (i.e., buoyancy driven transport) are conducted to show the interfacial instability. Depending on the relative magnitude of these two forces, the mixed fluid system can be characterized by the development of hydrodynamic instabilities causing perturbations in the hydraulic as well as in the concentration field of the mixed flow. These instabilities are of gravitational origin.

The rest of the paper is organized as follows. In the next section, we review the compositional governing equations. Then, in the third section, we choose the primary unknowns and present an iterative IMPES approach using these unknowns. In the fourth section, we report numerical experiments. Finally, we draw some concluding remarks in the last section.

2 Basic differential equations

We consider a compositional model under the assumptions that the flow process is isothermal (i.e., the constant temperature), the components form at most three phases (e.g., water, oil, and gas), there is no mass interchange between the water phase and the hydrocarbon phases (i.e., the oil and gas phases), and the diffusive effects are neglected.

Let ϕ and $\mathbf{k}$ denote the porosity and permeability of the porous medium $\Omega \subset \Re^3$, and S_α, μ_α, p_α, $\mathbf{u}_\alpha$, and $k_{r\alpha}$ be the saturation, viscosity, pressure, volumetric velocity, and relative permeability of the α phase, $\alpha = w, o, g$, respectively. Also, let ξ_{io} and ξ_{ig} represent the molar densities of component i in the oil (liquid) and gas (vapor) phases, respectively, $i = 1, 2, \ldots, N_c$, where N_c is the number of components. The molar density of phase α is given by

$$\xi_\alpha = \sum_{i=1}^{N_c} \xi_{i\alpha}, \quad \alpha = o,\ g. \tag{2.1}$$

The mole fraction of component i in phase α is then defined by $x_{i\alpha} = \xi_{i\alpha}/\xi_\alpha$, for $i = 1, \cdots, N_c$ and $\alpha = o, g$. The total mass is conserved for each component:

$$\frac{\partial(\phi\xi_w S_w)}{\partial t} + \nabla \cdot (\xi_w \mathbf{u}_w) = q_w, \tag{2.2a}$$

$$\frac{\partial(\phi[x_{io}\xi_o S_o + x_{ig}\xi_g S_g])}{\partial t} + \nabla \cdot (x_{io}\xi_o \mathbf{u}_o + x_{ig}\xi_g \mathbf{u}_g) = x_{io}q_o + x_{ig}q_g, \quad 1 \le i \le N_c, \tag{2.2b}$$

where ξ_w is the molar density of water and q_α stands for the flow rate of phase α at wells. In equation (2.2), the volumetric velocity $\mathbf{u}_\alpha$ is given by Darcy's law:

$$\mathbf{u}_\alpha = -\frac{k_{r\alpha}}{\mu_\alpha}\mathbf{k}\left(\nabla p_\alpha - \rho_\alpha \wp \nabla z\right), \qquad \alpha = w,\ o,\ g, \tag{2.3}$$

where ρ_α is the mass density of the α-phase, $\wp$ is the magnitude of the gravitational acceleration, and z is the depth. The mass flow rates of wells are given by Peaceman's

formulas [12]

$$q_\alpha = \sum_{k=1}^{N_w} \sum_{m=1}^{M_{wk}} \frac{2\pi \Delta z_{k,m}}{\ln(r_{e,k,m}/r_{c,k}) + s_{k,m}} \frac{\bar{k} k_{r\alpha} \rho_\alpha}{\mu_\alpha} \left[p_{bh,k} - p_\alpha - \rho_\alpha \wp (z_{w,k} - z) \right] \delta \left(\mathbf{x} - \mathbf{x}_{k,m} \right),$$

where $\delta(\mathbf{x} - \mathbf{x}_{k,m})$ is the Dirac delta function at $\mathbf{x}_{k,m}$, N_w is the total number of wells, $M_{w,k}$ is the total number of perforated zones of the kth well, $s_{k,m}$, $\Delta z_{k,m}$, and $\mathbf{x}_{k,m}$ are the skin factor, segment length, and central location of the mth perforated zone of the kth well, $r_{c,k}$ denotes the wellbore radius of the kth well, $r_{e,k,m}$ is the drainage radius of the kth well at the grid block in which $\mathbf{x}_{k,m}$ is located, respectively, $\bar{k}$ denotes some average of $\mathbf{k}$ at wells [12], and $p_{bh,k}$ is the bottom hole pressure of the kth well at datum $z_{w,k}$.

In addition to the differential equations (2.2) and (2.3), there are also algebraic constraints. The mole fraction balance implies that

$$\sum_{i=1}^{N_c} x_{io} = 1, \quad \sum_{i=1}^{N_c} x_{ig} = 1. \tag{2.4}$$

In the transport process, the saturation constraint reads

$$S_w + S_o + S_g = 1. \tag{2.5}$$

Finally, the phase pressures are related by capillary pressures

$$p_{cow} = p_o - p_w, \quad p_{cgo} = p_g - p_o. \tag{2.6}$$

Mass interchange between phases is characterized by the variation of mass distribution of each component in the oil and gas phases. As usual, these two phases are assumed to be in the phase equilibrium state at every moment. This is physically reasonable since the mass interchange between phases occurs much faster than the flow of porous media fluids. Consequently, the distribution of each hydrocarbon component into the two phases is subject to the condition of stable thermodynamic equilibrium, which is given by minimizing the Gibbs free energy of the compositional system [1, 6]:

$$f_{io}(p_o, x_{1o}, \ldots, x_{N_c o}) = f_{ig}(p_g, x_{1g}, \ldots, x_{N_c g}), \tag{2.7}$$

where f_{io} and f_{ig}, $1 \le i \le N_c$, are the fugacity functions of the ith component in the oil and gas phases, respectively.

Equations (2.2)–(2.7) provide $2N_c + 9$ independent relations, differential or algebraic, for the $2N_c + 9$ dependent variables: x_{io}, x_{ig}, $\mathbf{u}_\alpha$, p_α, and S_α, $\alpha = w, o, g$, $i = 1, \ldots, N_c$. With appropriate boundary and initial conditions, there is a closed differential system for these unknowns. For the convenience of presentation, set

$$p_{cw} = p_w - p_o, \quad p_{cg} = p_g - p_o; \tag{2.8}$$

i.e., $p_{cw} = -p_{cow}$ and $p_{cg} = p_{cgo}$. Moreover, for notational convenience, let $p_{co} = 0$. Several EOS (equations of state) can be used to define the fugacity functions f_{io} and f_{ig}, such as the Redlich-Kwong, Redlich-Kwong-Soave, and Peng-Robinson EOSs. Here we employ the most used Peng-Robinson EOS.

Define, for $\alpha = o, g$,

$$a_\alpha = \sum_{i=1}^{N_c}\sum_{j=1}^{N_c} x_{i\alpha}x_{j\alpha}(1-\kappa_{ij})\sqrt{a_i a_j}, \quad b_\alpha = \sum_{i=1}^{N_c} x_{i\alpha}b_i,$$

where κ_{ij} is a binary interaction coefficient between components i and j, and a_i and b_i are empirical factors for pure component i. The interaction coefficients account for molecular interactions between two unlike molecules. By definition, κ_{ij} is zero when i and j represent the same component, small when i and j represent components that do not differ much (e.g., when components i and j are both alkanes), and large when i and j represent components that are substantially different. Ideally, κ_{ij} depends on pressure and temperature and only on the identities of components i and j [15, 17].

The factors a_i and b_i can be computed by $a_i = \Omega_{ia}\alpha_i R^2 T_{ic}^2/p_{ic}$ and $b_i = \Omega_{ib}R\,T_{ic}/p_{ic}$, where R is the universal gas constant ($R = 0.8205$), T is the temperature, T_{ic} and p_{ic} are the critical temperature and pressure, the EOS parameters $\Omega_{ia} = 0.45724$ and $\Omega_{ib} = 0.07780$,

$$\alpha_i = \left(1-\lambda_i\left[1-\sqrt{T/T_{ic}}\right]\right)^2, \qquad \lambda_i = 0.375 + 1.542\omega_i - 0.27\omega_i^2,$$

and ω_i is the acentric factor for components i. The acentric factors roughly express the deviation of the shape of a molecule from a sphere [13]. We define

$$A_\alpha = \frac{a_\alpha p_\alpha}{R^2T^2}, \quad B_\alpha = \frac{b_\alpha p_\alpha}{R\,T}, \qquad \alpha = o, g, \tag{2.9}$$

where the pressure p_α is given by the Peng-Robinson two-parameter equation of state

$$p_\alpha = \frac{RT}{V_\alpha - b_\alpha} - \frac{a_\alpha}{V_\alpha(V_\alpha+b_\alpha)+b_\alpha(V_\alpha-b_\alpha)}, \tag{2.10}$$

with V_α being the molar volume of phase α. Introducing the compressibility factor

$$Z_\alpha = p_\alpha V_\alpha/(RT), \qquad \alpha = o, g, \tag{2.11}$$

then equation (2.10) can be expressed as a cubic equation in Z_α:

$$Z_\alpha^3 - (1-B_\alpha)Z_\alpha^2 + (A_\alpha - 2B_\alpha - 3B_\alpha^2)Z_\alpha - (A_\alpha B_\alpha - B_\alpha^2 - B_\alpha^3) = 0. \tag{2.12}$$

Now, for $i = 1, \ldots, N_c$ and $\alpha = o, g$, the fugacity coefficient $\varphi_{i\alpha}$ of component i in the mixture can be obtained from the equation

$$\begin{aligned}\ln\varphi_{i\alpha} = {} & \frac{b_i}{b_\alpha}(Z_\alpha - 1) - \ln(Z_\alpha - B_\alpha) \\ & -\frac{A_\alpha}{2\sqrt{2}B_\alpha}\left(\frac{2}{a_\alpha}\sum_{j=1}^{N_c} x_{j\alpha}(1-\kappa_{ij})\sqrt{a_i a_j} - \frac{b_i}{b_\alpha}\right)\ln\left(\frac{Z_\alpha + (1+\sqrt{2})B_\alpha}{Z_\alpha - (1-\sqrt{2})B_\alpha}\right).\end{aligned} \tag{2.13}$$

Finally, the fugacity of component i is defined by

$$f_{i\alpha} = p_\alpha x_{i\alpha} \varphi_{i\alpha}, \quad i = 1, \ldots, N_c, \ \alpha = o, g. \tag{2.14}$$

The distribution of each hydrocarbon component into the fluid and vapor phases is given by the thermodynamic equilibrium relation (2.7).

3 Iterative IMPES solution approach

When the IMPES is used within a Newton-Raphson iteration, we call it the iterative IMPES.

3.1 Choice of primary variables

As discussed in the previous section, equations (2.2)–(2.7) form a strongly coupled system of time-dependent, nonlinear differential equations, and algebraic constraints. While there are $2N_c + 9$ equations for the same number of dependent variables, this system can be written in terms of $2N_c + 2$ primary variables and other variables can be expressed as functions of them. The choice of these primary variables is very important. They must be carefully chosen so that main physical properties inherent in the governing equations and constraints are preserved, the nonlinearity and coupling among the equations are weakened, and efficient numerical methods for the solution of the resulting system can be devised.

To simplify the expressions in equation (2.2), we introduce some notation. We utilize the potentials

$$\Phi_\alpha = p_\alpha - \rho_\alpha \wp z, \qquad \alpha = w, o, g. \tag{3.1}$$

Also, we use the total mass variable F of the hydrocarbon system [11, 16]

$$F = \xi_o S_o + \xi_g S_g, \tag{3.2}$$

and the mass fractions of the oil and gas in this system

$$L = \xi_o S_o / F, \quad V = \xi_g S_g / F. \tag{3.3}$$

Note that $L + V = 1$. Next, instead of exploiting the individual mole fractions, we use the total mole fraction of the components in the hydrocarbon system

$$z_i = L x_{io} + (1 - L) x_{ig}, \qquad i = 1, \ldots, N_c. \tag{3.4}$$

Then it is easy to see, using (2.4), (3.2) and (3.3), that

$$\sum_{i=1}^{N_c} z_i = 1, \tag{3.5}$$

and $x_{io}\xi_o S_o + x_{ig}\xi_g S_g = Fz_i$, for $i = 1, \ldots, N_c$. Consequently, applying (2.3) and (3.1), the second equation of (2.2) becomes

$$\frac{\partial(\phi F z_i)}{\partial t} - \nabla \cdot \left(\mathbf{k}\left[x_{io}\xi_o k_{ro}\mu_o^{-1}\nabla\Phi_o + x_{ig}\xi_g k_{rg}\mu_g^{-1}\nabla\Phi_g\right]\right) = x_{io}q_o + x_{ig}q_g, \quad i = 1, \ldots, N_c. \tag{3.6}$$

Adding the equations in (3.6) over i and exploiting (2.4) and (3.5) give

$$\frac{\partial(\phi F)}{\partial t} - \nabla \cdot \left(\mathbf{k}\left[\xi_o k_{ro}\mu_o^{-1}\nabla\Phi_o + \xi_g k_{rg}\mu_g^{-1}\nabla\Phi_g\right]\right) = q_o + q_g. \tag{3.7}$$

Equation (3.6) is the individual flow equation for the ith component ($i = 1, \ldots, N_c - 1$) and equation (3.7) is the global hydrocarbon flow equation.

To simplify the differential equations further, we define the transmissibilities

$$\mathbf{T}_\alpha = \frac{\xi_\alpha k_{r\alpha}}{\mu_\alpha}\mathbf{k}, \qquad \mathbf{T}_{i\alpha} = \frac{x_{i\alpha}\xi_\alpha k_{r\alpha}}{\mu_\alpha}\mathbf{k}, \quad \alpha = o, g,\ i = 1, \cdots, N_c. \tag{3.8}$$

We now summarize the equations needed in the iterative IMPES. The equilibrium relation (2.7) is recast:

$$f_{io}(p_o, x_{1o}, \cdots, x_{N_c o}) = f_{ig}(p_o + p_{cg}, x_{1g}, \cdots, x_{N_c g}), \quad i = 1, \cdots, N_c. \tag{3.9}$$

Using (3.8), equation (3.6) becomes

$$\frac{\partial(\phi F z_i)}{\partial t} = \nabla \cdot (\mathbf{T}_{io}\nabla\Phi_o + \mathbf{T}_{ig}\nabla\Phi_g) + x_{io}q_o + x_{ig}q_g, \quad i = 1, \cdots, N_c - 1. \tag{3.10}$$

Similarly, it follows from (3.7) that

$$\frac{\partial(\phi F)}{\partial t} = \nabla \cdot (\mathbf{T}_o\nabla\Phi_o + \mathbf{T}_g\nabla\Phi_g) + q_o + q_g. \tag{3.11}$$

Next, applying the first equation of (2.2) and (3.8) yields

$$\frac{\partial(\phi\xi_w S_w)}{\partial t} = \nabla \cdot (\mathbf{T}_w\nabla\Phi_w) + q_w. \tag{3.12}$$

Finally, using (3.2) and (3.3), the saturation state equation (2.5) becomes

$$F\left(L\xi_o^{-1} + (1 - L)\xi_g^{-1}\right) + S = 1. \tag{3.13}$$

The differential system consists of the $2N_c + 2$ equations (3.9)–(3.13) for the $2N_c + 2$ primary unknowns: x_{io} (or x_{ig}), L (or V), z_i, F, $S = S_w$, and $p = p_o$, $i = 1, \cdots, N_c - 1$.

3.2 The iterative IMPES

Let $n > 0$ (an integer) refer to a time step. For any function v of space and time, we write $v^n(\cdot) = v(\cdot, t^n)$, and use $\bar{\delta}v$ to denote the time difference $\bar{\delta}v = v^{n+1} - v^n$. A time approximation at the $(n+1)$-th level for the system of equations (3.9)–(3.13) can be defined as follows:

$$f_{io}(p_o^{n+1}, x_{1o}^{n+1}, \cdots, x_{N_co}^{n+1}) = f_{ig}(p_g^{n+1}, x_{1g}^{n+1}, \cdots, x_{N_cg}^{n+1}), \qquad 1 \le i \le N_c, \tag{3.14a}$$

$$\frac{1}{\Delta t}\bar{\delta}(\phi F z_i) = \nabla \cdot (\mathbf{T}_{io}^{n+1}\nabla\Phi_o^{n+1} + \mathbf{T}_{ig}^{n+1}\nabla\Phi_g^{n+1}) + x_{io}^{n+1}q_o^{n+1} + x_{ig}^{n+1}q_g^{n+1}, \quad 1 \le i \le N_c - 1, \tag{3.14b}$$

$$\frac{1}{\Delta t}\bar{\delta}(\phi F) = \nabla \cdot (\mathbf{T}_o^{n+1}\nabla\Phi_o^{n+1} + \mathbf{T}_g^{n+1}\nabla\Phi_g^{n+1}) + q_o^{n+1} + q_g^{n+1}, \tag{3.14c}$$

$$\frac{1}{\Delta t}\bar{\delta}(\phi\xi_w S) = \nabla \cdot (\mathbf{T}_w^{n+1}\nabla\Phi_w^{n+1}) + q_w^{n+1}, \tag{3.14d}$$

$$\left[F\left(L\xi_o^{-1} + (1-L)\xi_g^{-1}\right) + S\right]^{n+1} = 1, \tag{3.14e}$$

where $\Delta t = t^{n+1} - t^n$. System (3.14) is nonlinear in the primary unknowns, and can be linearized via the Newton-Raphson iteration, for example. For function v, we set $v^{n+1,l+1} = v^{n+1,l} + \delta v$, where l refers to the number of Newton-Raphson's iteration and δv represents the increment in this iteration step. When no ambiguity occurs, we will write $v^{n+1,l+1}$ and $v^{n+1,l}$ by v^{l+1} and v^l, respectively (i.e., the superscript $n+1$ is omitted). Note that

$$v^{n+1} \approx v^{l+1} = v^l + \delta v,$$

so $\bar{\delta}v \approx v^l - v^n + \delta v$. Using this approximation in system (3.14) yields

$$f_{io}(p_o^{l+1}, x_{1o}^{l+1}, \cdots, x_{N_co}^{l+1}) = f_{ig}(p_g^{l+1}, x_{1g}^{l+1}, \cdots, x_{N_cg}^{l+1}), \quad 1 \le i \le N_c, \tag{3.15a}$$

$$\frac{1}{\Delta t}\left[(\phi F z_i)^l - (\phi F z_i)^n + \delta(\phi F z_i)\right] = \nabla \cdot (\mathbf{T}_{io}^{l+1}\nabla\Phi_o^{l+1} + \mathbf{T}_{ig}^{l+1}\nabla\Phi_g^{l+1}) + x_{io}^{l+1}q_o^{l+1} + x_{ig}^{l+1}q_g^{l+1}, \qquad 1 \le i \le N_c - 1, \tag{3.15b}$$

$$\frac{1}{\Delta t}\left[(\phi F)^l - (\phi F)^n + \delta(\phi F)\right] = \nabla \cdot (\mathbf{T}_o^{l+1}\nabla\Phi_o^{l+1} + \mathbf{T}_g^{l+1}\nabla\Phi_g^{l+1}) + q_o^{l+1} + q_g^{l+1}, \tag{3.15c}$$

$$\frac{1}{\Delta t}\left[(\phi\xi_w S)^l - (\phi\xi_w S)^n + \delta(\phi\xi_w S)\right] = \nabla \cdot (\mathbf{T}_w^{l+1}\nabla\Phi_w^{l+1}) + q_w^{l+1}, \tag{3.15d}$$

$$\left[F\left(L\xi_o^{-1} + (1-L)\xi_g^{-1}\right) + S\right]^{l+1} = 1. \tag{3.15e}$$

We expand the potentials and transmissibilities in terms of the primary unknowns. Toward that end, we need to identify these unknowns. If the gas phase dominates in the hydrocarbon system (e.g., $L < 0.5$), the primary unknowns will be x_{io}, L, z_i, F, S, and p, $i = 1, \cdots, N_c - 1$. That is, the so-called L-X iteration type is used. If the oil phase dominates (e.g., $L \ge 0.5$), the primary unknowns will be x_{ig}, V, z_i, F, S, and p, $i = 1, \cdots, N_c - 1$, which corresponds to the V-Y iteration type. As an example, we

illustrate how to expand the potentials and transmissibilities in terms of δx_{io}, δL, δz_i, δF, δS, and δp, $i = 1, \cdots, N_c - 1$; a similar expansion can be performed for the V-Y iteration type. For the ith component flow equation,

$$\delta(\phi F z_i) = c_{ip}\delta p + c_{iF}\delta F + c_{iz}\delta z_i, \quad i = 1, \cdots, N_c - 1, \tag{3.16}$$

where $c_{ip} = \phi^o c_R (F z_i)^l$, $c_{iF} = (\phi z_i)^l$ and $c_{iz} = (\phi F)^l$, with ϕ^o being the porosity at a reference pressure p^o and c_R the rock compressibility. For the global hydrocarbon flow equation,

$$\delta(\phi F) = c_p \delta p + c_F \delta F, \tag{3.17}$$

where $c_p = \phi^o c_R F^l$ and $c_F = \phi^l$. For the water flow equation,

$$\delta(\phi \xi_w S) = c_{wp}\delta p + c_{wS}\delta S, \tag{3.18}$$

where

$$c_{wp} = \phi^o c_R \left(\xi_w S\right)^l + \left(\phi \frac{d\xi_w}{dp} S\right)^l, \quad c_{wS} = \left(\phi \xi_w\right)^l.$$

In the iterative IMPES, all the saturation functions k_{rw}, k_{ro}, k_{rg}, p_{cw}, and p_{cg} are evaluated at the saturation values of the previous time step in Newton-Raphson's iteration, and the densities and viscosities in the transmissibilities, phase potentials, and well terms are computed using the previous Newton-Raphson iteration values. Thus the phase potentials are calculated by

$$\Phi_\alpha^{l+1} = p^{l+1} + p_{c\alpha}^n - \rho_\alpha^l \wp z, \qquad \alpha = w, o, g, \tag{3.19}$$

and the transmissibilities are computed by

$$\mathbf{T}_\alpha^{l+1} = \frac{\xi_\alpha^l k_{r\alpha}^n}{\mu_\alpha^l}\mathbf{k}, \quad \mathbf{T}_{i\alpha}^{l+1} = \frac{x_{i\alpha}^l \xi_\alpha^l k_{r\alpha}^n}{\mu_\alpha^l}\mathbf{k}, \quad \alpha = o, g,\ i = 1, \cdots, N_c. \tag{3.20}$$

It follows from (3.19) that

$$\Phi_\alpha^{l+1} = \Phi_\alpha^l + \delta p, \quad \alpha = w, o, g. \tag{3.21}$$

We now expand each of the equations in system (3.15). For this, we need to replace the derivatives in x_{ig} by those in the primary variables, $i = 1, \cdots, N_c$. Applying relation (3.4), we see that

$$\frac{\partial x_{ig}}{\partial x_{io}} = \frac{L}{L-1}, \quad \frac{\partial x_{ig}}{\partial z_i} = \frac{1}{1-L}, \quad \frac{\partial x_{ig}}{\partial L} = \frac{x_{io} - x_{ig}}{L-1}, \quad i = 1, \cdots, N_c.$$

Consequently, the chain rule implies

$$\frac{\partial}{\partial x_{io}} = \frac{\partial x_{ig}}{\partial x_{io}}\frac{\partial}{\partial x_{ig}} = \frac{L}{L-1}\frac{\partial}{\partial x_{ig}}, \qquad \frac{\partial}{\partial z_i} = \frac{\partial x_{ig}}{\partial z_i}\frac{\partial}{\partial x_{ig}} = \frac{1}{1-L}\frac{\partial}{\partial x_{ig}},$$
$$\frac{\partial}{\partial L} = \frac{\partial x_{ig}}{\partial L}\frac{\partial}{\partial x_{ig}} = \frac{x_{io} - x_{ig}}{L-1}\frac{\partial}{\partial x_{ig}}.$$

Thus, after using (2.4) and (3.5) to eliminate $x_{N_c o}$ and z_{N_c}, the first equation in (3.15) can be expanded as follows:

$$\begin{aligned}&\sum_{j=1}^{N_c-1}\left(w_o+L^l w_g/(1-L^l)\right)\delta x_{jo}+\frac{1}{1-L^l}\sum_{j=1}^{N_c}\left(\frac{\partial f_{ig}}{\partial x_{jg}}\left(x_{jo}-x_{jg}\right)\right)^l\delta L\\ =\;& f_{ig}^l-f_{io}^l+\left[\left(\frac{\partial f_{ig}}{\partial p}\right)^l-\left(\frac{\partial f_{io}}{\partial p}\right)^l\right]\delta p+\frac{1}{1-L^l}\sum_{j=1}^{N_c-1}w_g\delta z_j,\end{aligned}\tag{3.22}$$

where,

$$w_*=\left(\frac{\partial f_{i*}}{\partial x_{j*}}\right)^l-\left(\frac{\partial f_{i*}}{\partial x_{N_c*}}\right)^l,\quad *=o,g,\tag{3.23}$$

$f_{io}^l=f_{io}(p_o^l,x_{1o}^l,\cdots,x_{N_co}^l)$ and $f_{ig}^l=f_{ig}(p_g^l,x_{1g}^l,\cdots,x_{N_cg}^l)$, for $i=1,\cdots,N_c$. Equation (3.22) is used to solve for $(\delta x_{1o},\cdots,\delta x_{(N_c-1)o},\delta L)$ in terms of $(\delta z_1,\cdots,\delta z_{N_c-1},\delta p)$. Note that this equation is linear in $(\delta x_{1o},\cdots,\delta x_{(N_c-1)o},\delta L)$.

Next, applying (3.16) and (3.21), it follows that, from the second equation in (3.15) $i=1,\cdots,N_c-1$,

$$\begin{aligned}&\frac{1}{\Delta t}\left[(\phi F z_i)^l-(\phi F z_i)^n+c_{ip}\delta p+c_{iF}\delta F+c_{iz}\delta z_i\right]\\ &\quad=\nabla\cdot(\mathbf{T}_{io}^l\nabla\Phi_o^l+\mathbf{T}_{ig}^l\nabla\Phi_g^l)+\nabla\cdot\Big((\mathbf{T}_{io}^l+\mathbf{T}_{ig}^l)\nabla(\delta p)\Big)\\ &\qquad+\left(x_{io}^l+\delta x_{io}\right)q_o(\delta p,\delta p_{bh})+\Big(x_{ig}^l+\delta x_{ig}\Big)\,q_g(\delta p,\delta p_{bh}).\end{aligned}\tag{3.24}$$

Equation (3.24) is solved for $(\delta z_1,\delta z_2,\cdots,\delta z_{N_c-1})$ in terms of $(\delta F,\delta p,\delta p_{bh})$. Similarly, from the third equation in (3.15) we see that

$$\begin{aligned}&\frac{1}{\Delta t}\left[(\phi F)^l-(\phi F)^n+c_p\delta p+c_F\delta F\right]=\nabla\cdot(\mathbf{T}_o^l\nabla\Phi_o^l+\mathbf{T}_g^l\nabla\Phi_g^l)\\ &\quad+\nabla\cdot\big((\mathbf{T}_o^l+\mathbf{T}_g^l)\nabla(\delta p)\big)+q_o(\delta p,\delta p_{bh})+q_g(\delta p,\delta p_{bh}),\end{aligned}\tag{3.25}$$

which is employed to solve for δF in terms of δp and δp_{bh}. From the fourth equation in (3.15), (3.18) and (3.21), we have

$$\begin{aligned}&\frac{1}{\Delta t}\left[(\phi\xi_w S)^l-(\phi\xi_w S)^n+c_{wp}\delta p+c_{wS}\delta S\right]\\ =\;&\nabla\cdot(\mathbf{T}_w^l\nabla\Phi_w^l)+\nabla\cdot\Big(\mathbf{T}_w^l\nabla(\delta p)\Big)+q_w(\delta p,\delta p_{bh}).\end{aligned}\tag{3.26}$$

Equation (3.26) is utilized to obtain δS in terms of δp and δp_{bh}. It follows from (2.11) that

$$\frac{1}{\xi_\alpha}=\frac{1}{p_\alpha}Z_\alpha(p_\alpha,x_{1\alpha},\cdots,x_{N_c\alpha})RT,\qquad\alpha=o,g.$$

Then, applying (2.4) and (3.5), it follows from the last equation in (3.15) that

$$\begin{aligned}
&\left(\frac{FLRT}{p}\right)^l \sum_{j=1}^{N_c-1} (W_o - W_g)\,\delta x_{jo} + \left(\frac{FRT}{p}\right)^l \left[Z_o - Z_g - \sum_{j=1}^{N_c} \left(\frac{\partial Z_g}{\partial x_{jg}}\,(x_{jo} - x_{jg})\right)^l\right] \delta L \\
&\qquad + \left(\frac{FRT}{p}\right)^l \sum_{j=1}^{N_c-1} W_g \delta z_j + \left(\frac{RT}{p}\,(LZ_o + (1-L)Z_g)\right)^l \delta F + \delta S \\
&\qquad + \left(\frac{FRT}{p}\left[L\frac{\partial Z_o}{\partial p} - \frac{LZ_o}{p} + (1-L)\frac{\partial Z_g}{\partial p} - \frac{(1-L)Z_g}{p}\right]\right)^l \delta p \\
&\quad = 1 - \left(F\left[L/\xi_o + (1-L)/\xi_g\right] + S\right)^l, \qquad (3.27)
\end{aligned}$$

where

$$W_* = \left(\frac{\partial Z_*}{\partial x_{j*}}\right)^l - \left(\frac{\partial Z_*}{\partial x_{N_c*}}\right)^l, \qquad * = o, g. \qquad (3.28)$$

After substitution of δx_{jo}, δL, δz_j, δF and δS, $j = 1, \cdots, N_c - 1$ into (3.27) using equations (3.22)-(3.26), the resulting equation will become the pressure equation, which, together with the well control equations, is implicitly solved for δp and δp_{bh}. The CVFE introduced in the next section is applied to the discretization of equations (3.22)–(3.27).

In summary, the iterative IMPES for the compositional model has following features:

- The difference between the iterative IMPES and the classical IMPES is that the iterative IMPES is used within each Newton-Raphson iteration loop, while the classical one is utilized before the Newton-Raphson iteration procedure.
- All the saturation functions k_{rw}, k_{ro}, k_{rg}, p_{cw}, and p_{co} employ the previous time step values of saturation in Newton-Raphson's iteration.
- The densities and viscosities in the transmissibilities, phase potentials, and well terms are computed using the previous Newton-Raphson iteration values.
- The saturation constraint equation is used to solve implicitly for pressure p.
- The equilibrium relation is solved for $(x_{1o}, \cdots, x_{(N_c-1)o}, L)$.
- The ith component flow equation is utilized to obtain explicitly for $(z_1, \cdots, z_{N_c-1})$.
- The global hydrocarbon flow equation is exploited to solve explicitly for F.
- The water flow equation is explicitly solved for S.
- Relation (3.4) generates $(x_{1g}, \cdots, x_{N_c g})$.

3.3 Solution of equilibrium relation

In this section we discuss the solution for the thermodynamic equilibrium relation (3.9), which describes the mass distribution of each component in the oil and gas phases.

3.3.1 Successive substitution method

The equilibrium flash vaporization ratio for component i is defined by

$$K_i = x_{ig}/x_{io}, \qquad i = 1, \cdots, N_c, \tag{3.29}$$

where the quantity K_i is called the K-value of component i. If the iterative IMPES in the preceding section is used (i.e., the capillary pressure p_{cg} is evaluated at the previous time step value of saturation in Newton-Raphson's iteration), it follows from (2.14) that

$$f_{i\alpha} = p x_{i\alpha} \varphi_{i\alpha}, \quad i = 1, \cdots, N_c, \ \alpha = o, g. \tag{3.30}$$

Then, using (2.7), we see that $x_{io}\varphi_{io} = x_{ig}\varphi_{ig}$, $i = 1, \cdots, N_c$. Thus, by (3.29), we have

$$K_i = \varphi_{io}/\varphi_{ig}, \qquad i = 1, \cdots, N_c, \tag{3.31}$$

where the fugacity coefficients φ_{io} and φ_{ig} are defined in equation (2.13).

A *flash calculation* is an instant phase equilibrium: Given p, T, and z_i; and find L (or V), x_{io}, and x_{ig}, $i = 1, \cdots, N_c$. It follows from (3.4) and (3.29) that

$$\sum_{i=1}^{N_c} \frac{z_i(1-K_i)}{L + (1-L)K_i} = 0, \qquad x_{io} = \frac{z_i}{L + (1-L)K_i}, \quad i = 1, \cdots, N_c. \tag{3.32}$$

Based on (3.32), we introduce the following successive substitution method for the flash calculation:

- Initially, K_i is evaluated by the empirical formula

$$K_i = {p_{ir}}^{-1} \exp\left(5.3727(1+\omega_i)\left[1 - {T_{ir}}^{-1}\right]\right), \quad p_{ir} = p/p_{ic}, \ \ T_{ir} = T/T_{ic}.$$

- (F1) Given K_i and z_i, find L by using the following equation:

$$\sum_{i=1}^{N_c} \frac{z_i(1-K_i)}{L + (1-L)K_i} = 0;$$

- (F2) Find x_{io} and x_{ig} by

$$x_{io} = \frac{z_i}{L + (1-L)K_i}, \qquad x_{ig} = K_i x_{io}, \ \ i = 1, \ldots, N_c;$$

- (F3) Obtain K_i and z_i by

$$K_i = \varphi_{io}/\varphi_{ig}, \quad z_i = L x_{io} + (1-L)x_{ig}, \quad i = 1, \ldots, N_c.$$

- Return to (F1) and iterate until convergence.

In general, convergence of this successive substitution method is very slow. One can use the GDEM method to accelerate the convergence in the calculation of K_i:

$$\ln(K_i^{j+1}) = \ln(K_i^j) + \frac{\ln(K_i^j) - \ln(K_i^{j-1})}{1+\nu},$$

or equivalently

$$K_i^{j+1} = K_i^j \exp\left(\frac{\ln(K_i^j) - \ln(K_i^{j-1})}{1+\nu}\right),$$

where ν is the maximum characterization value

$$\nu = \frac{\left\langle \ln\left(K_i^j/K_i^{j-1}\right), \ln\left(K_i^{j-1}/K_i^{j-2}\right)\right\rangle}{\left\langle \ln\left(K_i^{j-1}/K_i^{j-2}\right), \ln\left(K_i^{j-1}/K_i^{j-2}\right)\right\rangle},$$

and j indicates the iteration number. This iteration proceeds until ν is constant.

In the neighborhood of a critical point (see Section 3.3.4), $\nu < 0$. In this case, one can use the RISNES method to accelerate the convergence in the calculation of K_i:

$$K_i^{j+1} = K_i^j \left(R_i^j\right)^{1/(1+\kappa)}, \quad \kappa = \frac{R_i^j - 1}{R_i^{j-1} - 1},$$

where $R_i^j = (f_{io}/f_{ig})^j = (K_i x_{io}/x_{ig})^j$, $i = 1, \ldots, N_c$. Again, this iteration proceeds until κ is constant.

3.3.2 Newton-Raphson flash calculation

As mentioned, convergence of the successive substitution method is very slow. One can employ the Newton-Raphson iteration in the flash calculation as in the iterative IMPES; see (3.22). Set

$$G_{ij} = w_o + + \frac{L^l}{1-L^l} w_g, \quad G_{iN_c} = \frac{1}{1-L^l} \sum_{j=1}^{N_c} \left(\frac{\partial f_{ig}}{\partial x_{jg}} (x_{jo} - x_{jg})\right)^l,$$

$$H_i(\delta p, \delta z_1, \cdots, \delta z_{N_c-1}) = f_{ig}^l - f_{io}^l + \left[\left(\frac{\partial f_{ig}}{\partial p}\right)^l - \left(\frac{\partial f_{io}}{\partial p}\right)^l\right] \delta p + \frac{1}{1-L^l} \sum_{j=1}^{N_c-1} w_g \delta z_j,$$

for $i = 1, \ldots, N_c$, $j = 1, \ldots, N_c - 1$, where w_* is defined by (3.23). Then equation (3.22) can be written in matrix form

$$\begin{pmatrix} G_{11} & G_{12} & \cdots & G_{1,N_c-1} & G_{1,N_c} \\ G_{21} & G_{22} & \cdots & G_{2,N_c-1} & G_{2,N_c} \\ \cdot & \cdot & \cdots & \cdot & \cdot \\ G_{N_c-1,1} & G_{N_c-1,2} & \cdots & G_{N_c-1,N_c-1} & G_{N_c-1,N_c} \\ G_{N_c,1} & G_{N_c,2} & \cdots & G_{N_c,N_c-1} & G_{N_c,N_c} \end{pmatrix} \begin{pmatrix} \delta x_{1o} \\ \delta x_{2o} \\ \cdot \\ \delta x_{(N_c-1)o} \\ \delta L \end{pmatrix} = \begin{pmatrix} H_1 \\ H_2 \\ \cdot \\ H_{N_c-1} \\ H_{N_c} \end{pmatrix}. \quad (3.33)$$

This system solves for $(\delta x_{1o}, \delta x_{2o}, \ldots, \delta x_{(N_c-1)o}, \delta L)$ in terms of δz_i and δp. One can use the forward Gauss elimination method to obtain an up-triangular system for (3.33).

We point out the difference between the successive substitution method and the Newton-Raphson iteration in the flash calculation.

- The former method is easier to implement and is more reliable, even near a critical point. However, its convergence is slower; it may take over 1,000 iterations near the critical point.
- The latter method is faster. But it needs a good initial guess for x_{io} and L, $i = 1, \ldots, N_c$; moreover, this method may difficultly converge near a critical point.
- These two methods can be combined. For example, the Newton-Raphson iteration can be utilized first, and when it is difficult to converge, the successive substitution method is employed.

3.3.3 Derivatives of fugacity coefficients

We calculate the partial derivatives involved in the Jacobian coefficient matrix of (3.33). First, by (3.30), one sees that, $i, j = 1, \ldots, N_c$, $\alpha = o, g$,

$$\frac{\partial f_{i\alpha}}{\partial p} = x_{i\alpha}\varphi_{i\alpha} + p x_{i\alpha}\frac{\partial \varphi_{i\alpha}}{\partial p}, \quad \frac{\partial f_{i\alpha}}{\partial x_{j\alpha}} = p\frac{\partial x_{i\alpha}}{\partial x_{j\alpha}}\varphi_{i\alpha} + p x_{i\alpha}\frac{\partial \varphi_{i\alpha}}{\partial x_{j\alpha}},$$

where

$$\frac{\partial x_{i\alpha}}{\partial x_{j\alpha}} = \begin{cases} 1 & \text{if } i = j, \\ 0 & \text{if } i \neq j. \end{cases}$$

As a result, it suffices to find the derivatives of $\varphi_{i\alpha}$, which is defined by (2.13). It follows from (2.9) that

$$\frac{\partial A_\alpha}{\partial p} = \frac{a_\alpha}{R^2T^2}, \quad \frac{\partial B_\alpha}{\partial p} = \frac{b_\alpha}{RT}, \quad \alpha = o, g. \tag{3.34}$$

Then differentiating both sides of (2.13) gives

$$\begin{aligned} \frac{1}{\varphi_{i\alpha}}\frac{\partial \varphi_{i\alpha}}{\partial p} &= \frac{b_i}{b_\alpha}\frac{\partial Z_\alpha}{\partial p} - \frac{1}{Z_\alpha - B_\alpha}\left(\frac{\partial Z_\alpha}{\partial p} - \frac{B_\alpha}{p}\right) \\ &\quad - \frac{A_\alpha}{2\sqrt{2}B_\alpha}\left(\frac{2}{a_\alpha}\sum_{j=1}^{N_c} x_{j\alpha}(1-\kappa_{ij})\sqrt{a_i a_j} - b_i/b_\alpha\right)\cdot 2\frac{B_\alpha}{\beta_\alpha}\left(\frac{Z_\alpha}{p} - \frac{\partial Z_\alpha}{\partial p}\right), \end{aligned} \tag{3.35}$$

where $\beta_\alpha = Z_\alpha^2 + 2\sqrt{2}Z_\alpha B_\alpha + B_\alpha^2$. Similarly, we can obtain $\partial\varphi_{i\alpha}/\partial x_{j\alpha}$ using the following expressions:

$$\begin{aligned} &\frac{\partial A_\alpha}{\partial x_{j\alpha}} = \frac{p}{R^2T^2}\frac{\partial a_\alpha}{\partial x_{j\alpha}}, \quad \frac{\partial B_\alpha}{\partial x_{j\alpha}} = \frac{p}{R\,T}\frac{\partial b_\alpha}{\partial x_{j\alpha}}, \\ &\frac{\partial a_\alpha}{\partial x_{j\alpha}} = 2\sum_{i=1}^{N_c} x_{i\alpha}(1-\kappa_{ij})\sqrt{a_i a_j}, \quad \frac{\partial b_\alpha}{\partial x_{j\alpha}} = b_j, \end{aligned} \tag{3.36}$$

for $i,j=1,\ldots,N_c$, $\alpha=o,g$. The Z-factors, Z_α ($\alpha=o,g$), are determined by equation (2.12), which can be exploited to find their derivatives. An application of the implicit differentiation to (2.12) yields

$$\frac{\partial Z_\alpha}{\partial p}=-\left\{\frac{\partial B_\alpha}{\partial p}Z_\alpha^2+\left(\frac{\partial A_\alpha}{\partial p}-2\left[1+3B_\alpha\right]\frac{\partial B_\alpha}{\partial p}\right)Z_\alpha \\ -\left(\frac{\partial A_\alpha}{\partial p}B_\alpha+\gamma_\alpha\frac{\partial B_\alpha}{\partial p}\right)\right\}/\left(2Z_\alpha^2-2(1-B_\alpha)Z_\alpha+\gamma_\alpha\right), \tag{3.37}$$

where $\gamma_\alpha=A_\alpha-2B_\alpha-3B_\alpha^2$. Consequently, substitution of (3.34) into (3.37) gives $\partial Z_\alpha/\partial p$. A similar argument, together with (3.36), computes the derivatives $\partial Z_\alpha/\partial x_{j\alpha}$, $j=1,\ldots,N_c$.

3.3.4 Practical considerations

We point out a few practical issues in programming.

`Iteration switch.` As noted, depending on the size of L, different variables, either x_{io} and L or x_{ig} and V, should be used in the flash calculation, $i=1,\ldots,N_c$. If the gas phase dominates in the hydrocarbon system (e.g., $L<0.5$), the primary unknowns will be x_{io} and L. If the oil phase dominates (e.g., $L\geq 0.5$), the primary unknowns will be x_{ig} and V. This choice can improve solution accuracy and convergence speed. For example, as L gets close to one, the flash calculation may not converge. In this case, the primary unknown needs to switch to V. In programming, the switch of iterations should be done automatically.

`Determination of bubble points.` The following system of N_c+1 equations are solved simultaneously for pressure p (bubble point pressure) and compositions x_{ig} by the Newton-Raphson iteration:

$$z_i\varphi_{io}=x_{ig}\varphi_{ig},\quad i=1,\ldots,N_c,\quad \sum_{i=1}^{N_c}x_{ig}=1. \tag{3.38}$$

In the late Newton-Raphson iterations (e.g., after ten iterations), the second equation in (3.38) can be replaced by

$$\sum_{i=1}^{N_c}\varphi_{io}/\varphi_{ig}z_i=1. \tag{3.39}$$

In the iteration process, if the successive values of pressure change less than 0.01 psi, this iteration process is said to converge. The process fails to converge if more than 30 iterations are used or if $|z_i-x_{ig}|<0.001|z_i|$. In the latter case, the successive substitution method can be utilized to obtain p and x_{ig}, $i=1,\ldots,N_c$. A trivial solution occurs when $x_{ig}=z_i$ for any value of p, indicating that a dew point occurs. In the Newton-Raphson iteration, the equations in (3.38) (or (3.39)) can be expanded as in the iterative IMPES.

`Determination of dew points.` The dew point pressure p and the compositions x_{io} satisfy the system of $N_c + 1$ equations

$$x_{io}\varphi_{io} = z_i\varphi_{ig}, \quad i = 1, \ldots, N_c, \quad \sum_{i=1}^{N_c} x_{io} = 1. \tag{3.40}$$

Again, after ten Newton-Raphson's iterations, the second equation in (3.40) is replaced by

$$\sum_{i=1}^{N_c} \varphi_{ig}/\varphi_{io}z_i = 1. \tag{3.41}$$

Using the same guideline as in the treatment of bubble points, if the successive values of pressure in the iteration process change less than 0.01 psi, this process is said to converge. The convergence fails if more than 30 iterations are employed or if $|z_i - x_{io}| < 0.001|z_i|$. In the latter case, the successive substitution method can be utilized to obtain p and x_{io}, $i = 1, 2, \ldots, N_c$. A trivial solution occurs when $x_{io} = z_i$ for any value of p, indicating that a bubble point occurs.

4 Numerical results

The compositional model presented in the previous section is now applied to the numerical study of the nonlinear evolution of interfaces between two miscible fluids of different densities. Special emphasis is placed on studying the influence of free convection, forced convection, diffusion/dispersion, and Peclet numbers on the interfacial instabilities under gravitational forces. Finite volume methods are used for the spacial discretization of the model equations, an implicit second-order integration scheme is exploited for time differentiation terms, the Newton-Raphson iteration is utilized for linearization, and the BiCGSTAB iterative algorithm with ILU preconditioners is employed for the solution of linear systems. The finite volume methods used are of second-order accuracy in both time and space for the concentrations [2].

4.1 Free convection

This is a free convection system where we start with a heavier fluid on top and a lighter fluid in bottom (no diffusion). The initial concentrations are given in Fig. 1(a). The physical data are: The domain Ω is a two-dimensional homogeneous medium with a no-flow boundary condition, the permeability is $5.6e^{-4}$, the porosity is 0.38, and the relative density and viscosity are 0.02 and 0.35, respectively. The grid-point number is of order 100 in each horizontal direction. The concentration contours at two different times are shown in Figs. 1(b) and 1(c). From these figures, we see that the mean flow is influenced by the average density gradients causing descent of the heavier fluid. There is also a local region near the lower edge of the heavier fluid in which this fluid overlies the lighter one resulting in a system that is gravitational unstable.

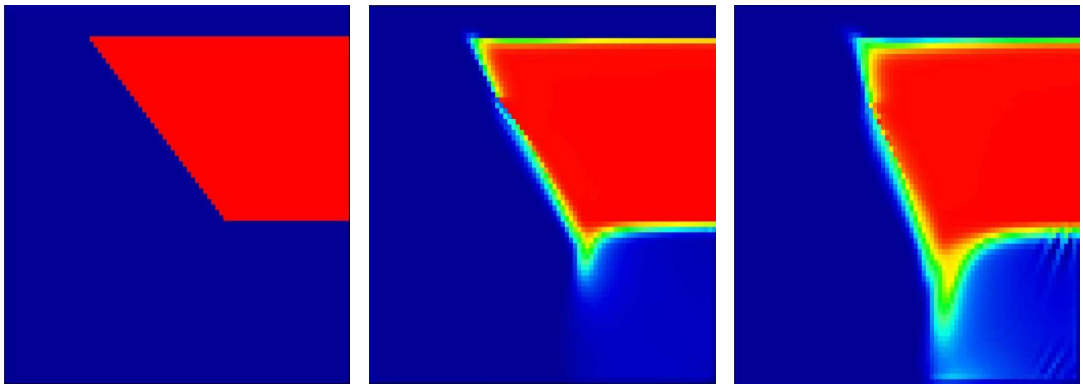

(a) Initial time (b) A later time (c) Another later time

Figure 1: Concentration for a free convection system in three different times.

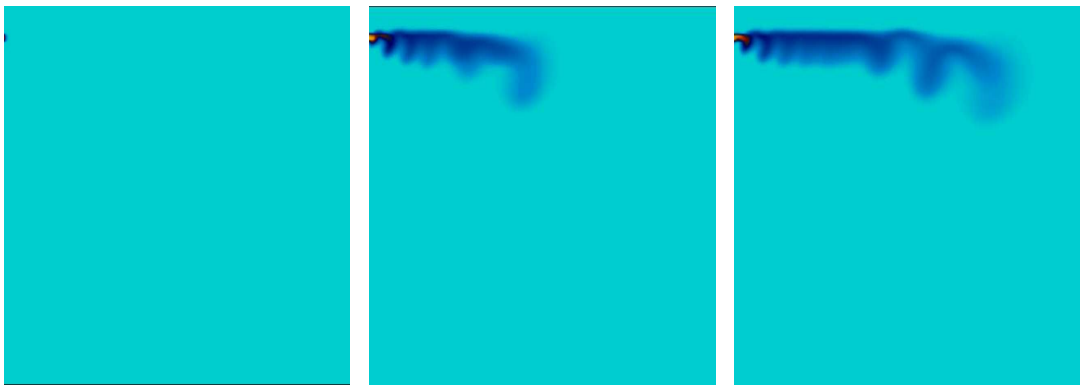

(a) Time 1. (b) Time 2. (c) Time 3.

Figure 2: Concentration for a forced convection system in three different times.

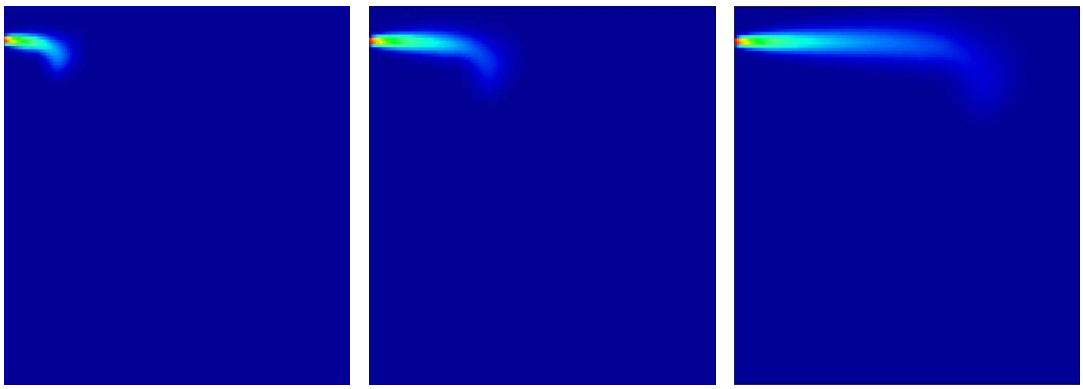

(a) Time 1. (b) Time 2. (c) Time 3

Figure 3: Concentration for a forced convection/dispersion system in three different times.

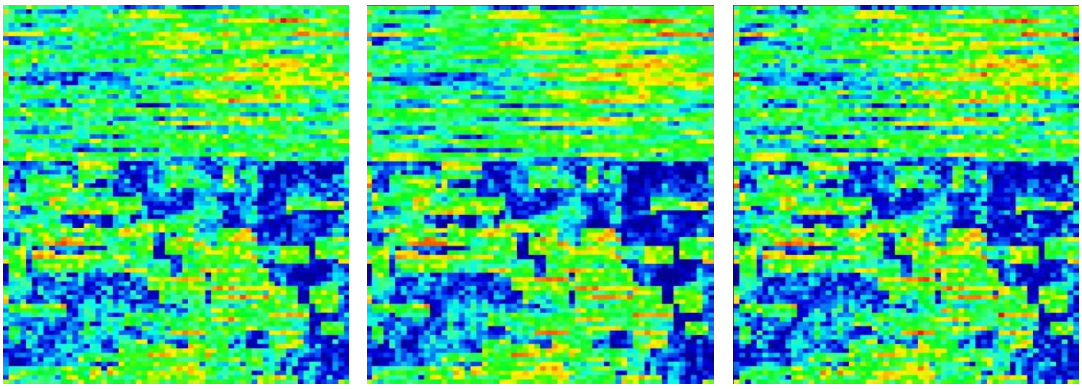

(a) Porosity (b) Horizontal permeability (c) Vertical permeability

Figure 4: Porosity, horizontal and vertical permeability.

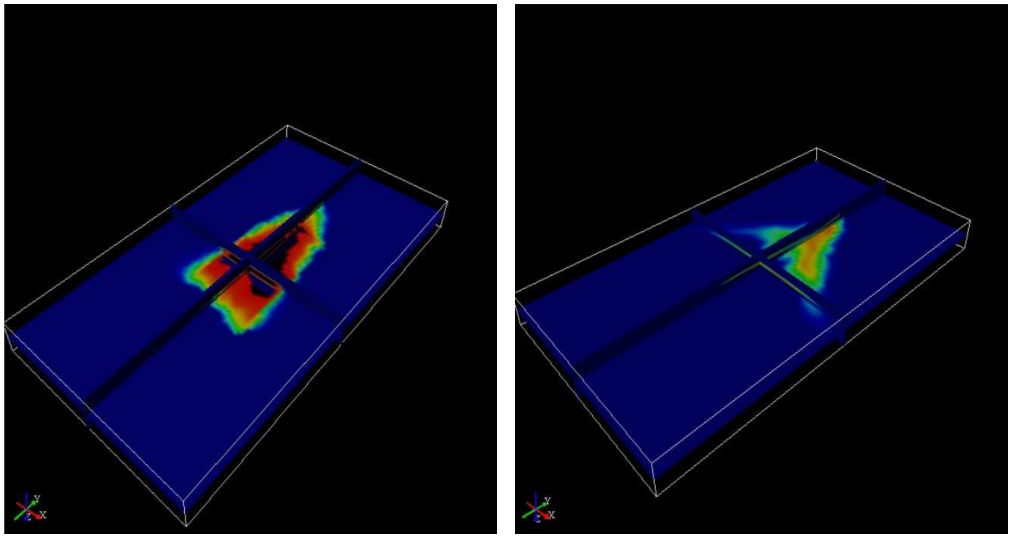

(a) Time 1. (b) Time 2.

Figure 5: Concentration for a three-dimensional heterogeneous medium in two different times.

4.2 Forced convection

This is a forced convection system where we inject a heavier component into a fluid which consists entirely of a lighter component without diffusion. The physical data are the same as in the free convection case except that the left and right boundaries are now given with a constant velocity. Three concentration contours at three different times are illustrated in Fig. 2. The interfacial instabilities are of the form of lobe-shaped protuberances that manifested themselves near the lower edge of the plume. As they develop spatially and temporally, they penetrate deeper and deeper into the plume, resulting in considerable modification to the overall dispersion.

4.3 Forced convection plus dispersion

This is now a forced convection system with dispersion. The Peclet number (characteristic speed and length divided by diffusion/dispersion) equals 5,000, and the longitudinal and transverse dispersion coefficients are, respectively, $0.031e^{-2}$ and $0.00217e^{-2}$. Three concentration contours at three different times are presented in Fig. 3.

There are two basic processes operating to transport chemical species. Diffusion is the process by which both ionic and molecular species dissolved in a fluid phase (e.g., water) move from areas of higher concentration (i.e., chemical activity) to areas of lower concentration. Advection is the process by which the moving fluid phase carries with it dissolved species. The process of dispersion acts to dilute the species and lower its concentration of movement so that it may not move as fast as the advection rate indicates.

If the transverse dispersion is too low, the movement remains narrow and stable. On the other hand, if the value is too high, the movement spreads rapidly and again remains stable. It is only at some intermediate values between these two extremes that instability appears.

4.4 Forced convection in a heterogeneous porous medium

In the last example, we simulate a forced convection system with dispersion in a three-dimensional heterogeneous porous medium. The physical data are: A no-flow boundary condition is imposed at the bottom of the domain, all other boundaries are of Dirichlet type, the Peclet number is 5,000, the relative density and viscosity are 0.02 and 0.35, and the longitudinal and transverse dispersion coefficients are $0.031e^{-2}$ and $0.00217e^{-2}$, respectively. The porosity, the horizontal and vertical permeabilities are shown in Fig. 4. Two concentrations in three dimensions are presented in Fig. 5. Observations similar to those made in the previous example can be made here.

5 Concluding remarks

The main contributions of this paper are to develop an iterative IMPES solution approach for the numerical simulation of three-dimensional, multiphase, multicomponent compositional flow in porous media, to apply it for the study of the nonlinear evolution of interfaces between miscible fluids of different densities, and to develop a high-order finite volume method for numerical solution of the compositional model. Extensive numerical experiments have been presented. Fluid mixing is the process of diffusion across interfacial surfaces to produce fluid of intermediate density and is irreversible. Instability is governed by the magnitude of the horizontal flow velocity, fluid injection rate, and the density difference. Density differences influence the flow primarily by establishing a narrow gravity layer in which the effective Peclet number is enhanced owing to the higher flow rate. However, buoyancy forces of a certain magnitude can lead to a pinch-off of the gravity layer, thereby slowing it down. Overall, an increase of the gravitational parameter

is found to enhance mostly the vertical perturbation, while larger Peclet values act towards amplifying horizontal disturbances.

References

[1] J. Bear, Dynamics of Fluids in Porous Media, Dover, New York, 1972.
[2] Z. Chen, The control volume finite element methods and their applications to multiphase flow, Networks and Heterogeneous Media, to appear.
[3] Z. Chen, R. E. Ewing and Z.-C. Shi (Eds.), Numerical Treatment of Multiphase Flows in Porous Media, Lect. Notes Phys., Vol. 552, Springer-Verlag, Heidelberg, 2000.
[4] Z. Chen, G. Huan and H. Wang, Simulation of a compositional model for multiphase flow in porous media, Numer. Meth. Part. Diff. Eq., 21 (2005), 726–741.
[5] Z. Chen, G. Huan and H. Wang, Simulation of gas cycling of retrograde condensate reservoirs using an unstructured CVFE compositional model, Computing, to appear.
[6] Z. Chen, G. Qin and R. E. Ewing, Analysis of a compositional model for fluid flow in porous media, SIAM J. Appl. Math., 60 (2000), 747–777.
[7] Douglas, Jr., J., D. W. Peaceman and H H. Rachford, Jr. A method for calculating multi-dimensional immiscible displacement, Trans. AIME, 216 (1959), 297–306.
[8] R. E. Ewing (Ed.), The Mathematics of Reservoir Simulation, SIAM, Philadelphia, 1983.
[9] G. M. Homsy, Viscous fingering in porous media, Ann. Rev. Fluid Mech., 19 (1987), 271–280.
[10] R.C. MacDonald and K.H. Coats, Methods for numerical simulation of water and gas coning, Trans. AIME, 249 (1970), 425–436.
[11] J. S. Nolen, Numerical simulation of compositional phenomena in petroleum reservoirs, Reprint Series, SPE, Dallas, 11 (1973), 268–284.
[12] D.W. Peaceman, Interpretation of well-block pressures in numerical reservoir simulation, SPE 6893, 52nd Annual Fall Technical Conference and Exhibition, Denver, 1977.
[13] R. C. Reid, J. M. Prausnitz and T. K. Sherwood, The Properties of Gases and Liquids, third edition, St. Louis, McGraw-Hill, 1977.
[14] J. A. Trangenstein and J. B. Bell, Mathematical structure of compositional reservoir simulation, SIAM J. Sci. Stat. Comput., 10 (1989), 817–845.
[15] C. H. Whitson, Effect of physical properties estimation on equation-of-state predictions, paper SPE 11200, presented at the 57th Annual Fall Technical Conference and Exhibition of the Society of Petroleum Engineers of AIME, New Orleans, Louisiana, 1982.
[16] L. C. Young and R. E. Stephenson, A generalized compositional approach for reservoir simulation, Soc. Pet. Eng. J., 23 (1983), 727–742.
[17] D. Zudkevitch and J. Joffe, Correlation and prediction of vapor-liquid equilibria with the Redlich-Kwong equation of state, AIChE J., 16 (1970), 112–199.